NUMERICAL ANALYSIS OF AIR TEMPERATURE INCREASES IN URBAN AREA USING THE BUILDING-URBAN-SOIL SIMULTANEOUS SIMULATION MODEL

Aya Hagishima, Jun Tanimoto and Tadahisa Katayama
Department of Energy and Environmental Engineering,
Interdisciplinary Graduate School of Engineering Sciences, Kyushu University
6-1, Kasuga-koen, Kasuga-shi, +816-8580, -Japan

ABSTRACT

The authors propose a predicting methodology combined with simultaneous solution for Building-Urban-Soil system to analyze the heat island phenomenon quantitatively in this paper.
Using this model, numerical simulation is performed in order to analyze quantitative effects of many factors on the heat island phenomenon. The factors of the heat island phenomenon addressed are: ground materials, geometric urban configuration, artificial exhausted heat release, physical properties of buildings envelope and mechanical performance of air-conditioning system.

INTRODUCTION

Significant air temperature increases in urban areas is well known as the heat island phenomenon in a global scale. It is qualitatively grasped so far that both increase of anthropogenic heat and alteration of land usage are regarded as its main factors. To mitigate the heat island phenomenon, many studies have been carried out. Reviewing those former studies, their standpoints can be classified into two main groups:
(1) Empirical studies focused on trying to utilize natural heat sinks such as river, pond, green space, sea breeze and roof garden
(2) Numerical studies concerned on three-dimensional turbulent model to predict urban climate

Consequences from the former approach seem to be insufficient to supply significant backgrounds for urban planning and architectural designing because most of them remain at qualitative viewpoint. The second approach has not yet sufficiently reached to quantitative analysis to confirm factors of the heat island phenomenon, because their huge computational load causes following problems:
- Calculation procedure of radiative and evaporative heat transfer at buildings and soil surfaces are much simplified, so then, it is impossible to analyze exactly quantitative effects on the heat island phenomenon.
- It is very difficult to perform a large number of numerical experiment, therefore general and objective conclusion can not be obtained.

Under those circumstances, we propose a predicting methodology of the heat island phenomenon combined with simultaneous solution for Building-Urban-Soil system (BUSSSM) which is capable to analyze quantitatively the heat island phenomenon. Using BUSSSM, we performed a series of numerical experiment of which results were possible to lead to quantitative discussion about prime factors of the heat island phenomenon.

FEATURES OF BUSSSM

Grid pattern with buildings of same scale is assumed in an urban area as indicated in Figure 1. The horizontal advection is ignored. Figure 2 shows the features of BUSSSM.

BUSSSM is composed of several sub-models concentrated in thermal behavior of building, evaporation from soil surface, evapotranspiration from vegetation and manner of atmosphere respectively. Each sub-model stands on one-dimensional energy and mass conservation principles. In practical calculation process BUSSSM runs with all sub-models, which means whole of BUSSSM are treated as a simultaneous non-linear system.

Although one-dimensional model is not adequate for predicting urban microclimate in specified area like a so-called case study, it is more appropriate to deal with imaginary or typical urban areas. In addition, numerical solution by one-dimensional model requires smaller computation than that by three-dimensional model, therefore it will be more moderate to plunge into complex and simultaneous problems.

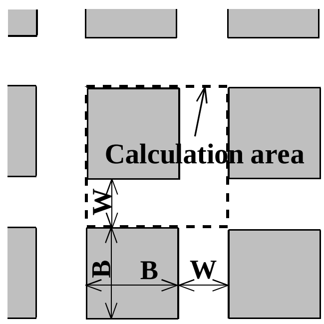

Fig.1 Grid pattern of urban area in BUSSSM

URBAN SUB-MODEL

Urban sub-model deals with one-dimensional vertical profile of wind velocity, temperature and humidity in urban atmosphere, which is described by following momentum, heat and vapor transfer equations.

$$m\frac{\partial u}{\partial t}=\frac{\partial\left(K_m\cdot m\frac{\partial u}{\partial z}\right)}{\partial z}-F_{ri}\cdots\cdots(1)$$

$$m\frac{\partial \theta}{\partial t}=\frac{\partial\left(K_h\cdot m\frac{\partial \theta}{\partial z}\right)}{\partial z}+H\cdots\cdots(2)$$

$$m\frac{\partial x}{\partial t}=\frac{\partial\left(K_v\cdot m\frac{\partial x}{\partial z}\right)}{\partial z}+W\cdots\cdots(3)$$

where u, θ and x are the wind velocity, the potential temperature and the absolute humidity respectively. F_{ri}, H and W are source terms. m is the ratio of volume density of fluid.

$$m=1-\left(\frac{B}{B+W}\right)^2,(z\leq H)\cdots\cdots(4)$$

K_m, K_h and K_v are eddy diffusivity can be written as followings (Pielke 1990):

$$K_m=K_h=K_v=1.1\left(\frac{Ric-Ri}{Ric}\right)l^2\left|\frac{\partial u}{\partial z}\right|,(Ri\leq Ric)\cdots\cdots(5)$$

$$K_m=K_h=K_v=l^2\left|\frac{\partial u}{\partial z}\right|,(Ri\geq Ric)\cdots\cdots(6)$$

where Ri is Richardson number, Ric is critical Richardson number (=0.25), l is mixing length.
Mass force F_{ri} due to buildings resistance can be expressed as:

$$F_{ri}=\frac{1}{2}c\cdot a\cdot u^2\cdots\cdots(7)$$

where a is building area projecting perpendicular to wind direction, c is resistance coefficient. Maruyama experimentally verified Eq.7 for staggered street pattern, meanwhile adopting 2-dimensional k-ε model calculation(Maruyama 1989).

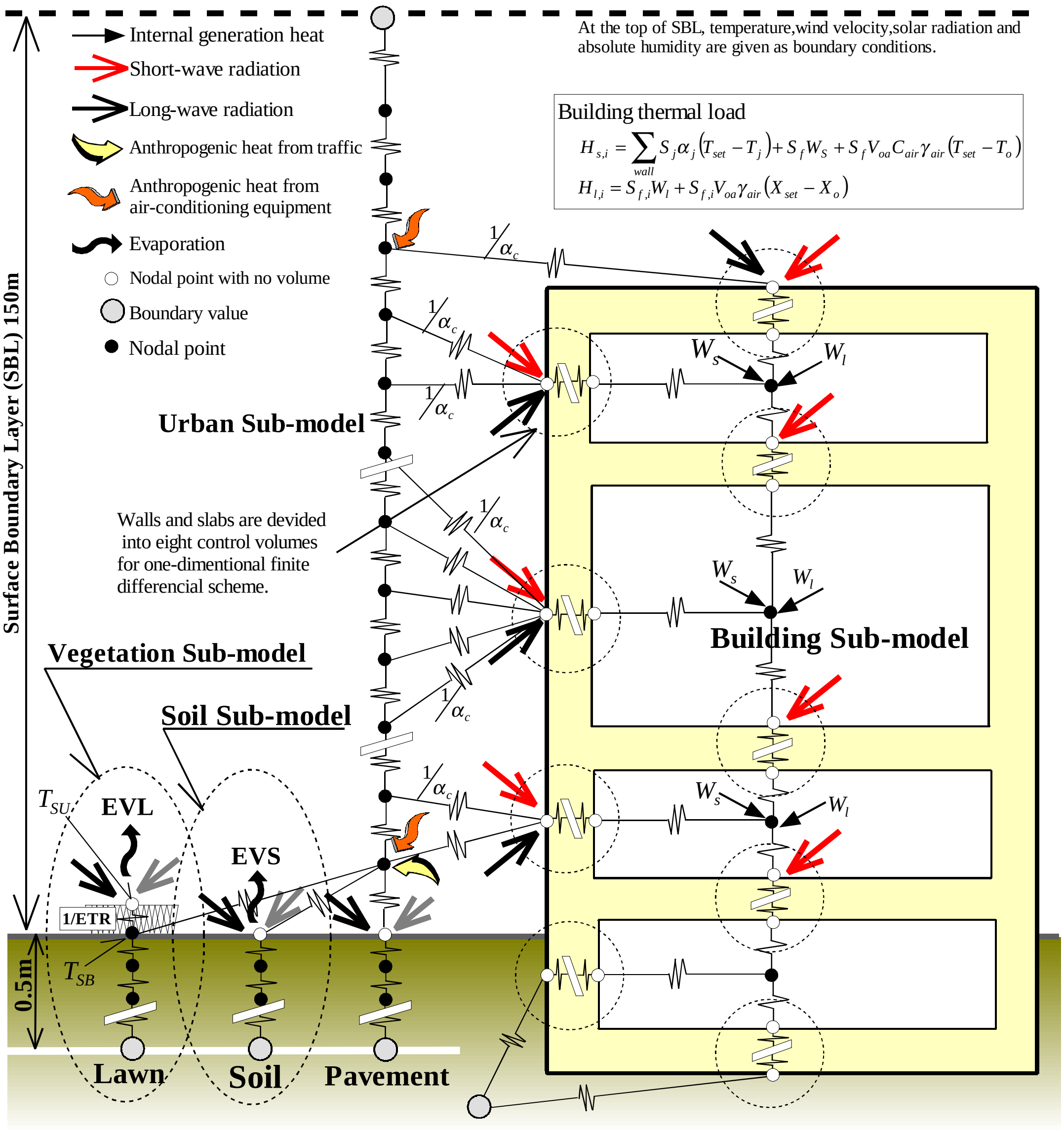

Fig.2 Schematic chart for heat balances in BUSSSM

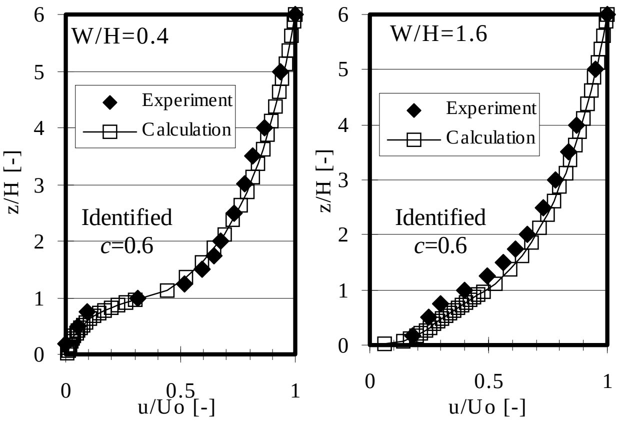

Fig.3 Comparison of wind profiles between calculation and experiment

However, there is no validation about the one-dimensional model combined with Eq.7 for normal street pattern, which is basic configuration of an urban area in BUSSSM. Therefore, we performed wind tunnel experiment and identified the resistance coefficient *c*.

Figure 3 shows the comparison of wind profiles between calculation and experiment. Considering simplicity of the model itself, agreement with the experiment is supposed to be satisfied.

SOIL SUB-MODEL TO PREDICT EVAPORATION FROM GROUND SURFACE

This sub-model is the simplified empirical procedure to evaluate fluctuation of evaporative efficiency of soil due to wetness of plow layer of which depth is determined 0.3m from soil surface. The water balance equation at the plow layer is expressed as (Tanimoto 1997):

$$\gamma_s \cdot \Delta x \frac{d\phi}{dt} = P - EVS - GD(\phi) + C \cdots\cdots\cdots (8a)$$

$$\phi \leq \phi_{sat} \cdots\cdots\cdots\cdots\cdots\cdots\cdots\cdots\cdots\cdots\cdots\cdots\cdots (8b)$$

ϕ is weight water content ratio of the soil and ϕ_{SAT} is saturated water content ratio. ΔX is determined 0.3m uniquely. γ_S is specific weight of the soil.

$$\gamma_s = (1-\phi)^{-1} \cdot \gamma_{dry} \cdots\cdots\cdots (9)$$

γ_{dry} is the specific weight of the soil in absolute dry condition. *P* is the precipitation term, *EVS* is the evaporation term. *C* and *GD* are the diffusion term and water transfer due to gravity between plow layer and underneath respectively.

EVS can be written as:

$$EVS = re(\phi/\phi_{SAT}) \cdot \frac{\alpha_C}{C_P} \cdot \left(X_{surf} - X_{air}\right) \cdots\cdots (10)$$

where *re* is the evaporation ratio. X_{air} is air absolute humidity, X_{surf} is saturated absolute humidity defined by soil surface temperature. α_c is convective heat transfer coefficient and C_p is specific heat of humid air. *GD* and *re* are expressed as functions of weight water content of the plow layer. Those characteristic are obtained from the experiments of authors in which four kinds of soil were identified,

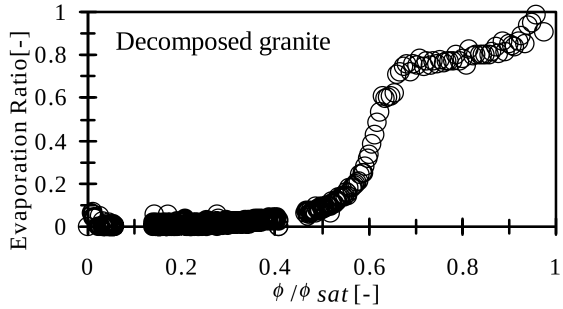

Fig.4 Relationship between evaporation ratio and normalized weight water content of plow layer

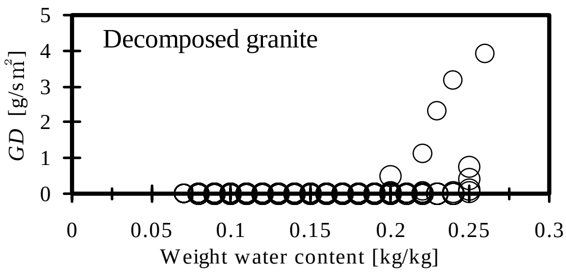

Fig.5 Relationship between permeance term *GD* and weight water content of plow layer

one of them are shown in Figure 4 and Figure 5 (Tanimoto 1997, Kawakami 1998). In this paper, *C* of decomposed granite is assumed zero provisionally. The validity of this model was also tested experimentally. This method can reduce calculation load exceedingly compared with the conventional procedure based on the simultaneous hygrothermal transfer equations.

VEGETATION SUB-MODEL TO PREDICT EVAPOTRANSPIRATION FROM LAWN

This is the model to evaluate evaporative efficiency from lawn based on a series of measurement data (Kagawa 1998). The heat balance equation at lawn surface can be written as:

$$SR + LR + CD + CV + EVL = 0 \cdots\cdots\cdots\cdots\cdots (11)$$

$$CD = \frac{1}{ETR}\left(T_{SB} - T_{SU}\right) \cdots\cdots\cdots\cdots\cdots\cdots\cdots\cdots\cdots (12)$$

SR and *LR* represent solar radiation and long-wave radiation, respectively. *CD* and *CV* are the conduction term and convection term. *ETR* is the equivalent thermal resistance of the layer of lawn leaves. T_{SB} and T_{SU} represent the temperatures of lawn surface and of lawn root.

The evaporation term *EVL* can be written as:

$$EVL = \kappa \cdot EVS \cdots\cdots\cdots\cdots\cdots\cdots\cdots\cdots\cdots\cdots (13)$$

κ is the evaporation ratio of lawn with soil to bare soil which is expressed as a function of volumetric water content of bare soil under the same condition. *ETR* and κ are determined by a large number of outdoor experimental data during over a year observation which was also presented schematically in the former mentioned article.

BUILDING SUB-MODEL

Building sub-model is almost based on the usual methodology to predict building thermal load. Imaginary deformed three-storied building with basement is presumed, of which middle story represents several stories. (see Figure 2)

Surface temperatures of every wall at each direction and every floor are deduced from discreted nodal one-dimensional heat transfer equation considering every boundary condition but evaporation.
Multiple reflections of both solar radiation and long-wave radiation are calculated by the radiosity method.

Building and road surfaces are divided into several rectangles for convenient consideration. Those surfaces are assumed as perfect diffusers. Solar transmittance and reflectance of the glazing are defined by solar incident angle.
Building sensible heat load *Hs* is expressed as:

$$H_S = \sum_{4directions} S_j \cdot \alpha_j \cdot (T_{set} - T_{S,j}) + S_f W_S + S_f V_{oa} C_{air} \gamma_{air} (T_{set} - T_o) \cdots\cdots\cdots\cdots (14)$$

W_s represents the internal sensible heat generation. S_j and S_f are the area of the wall and that of the floor. α_j is the convective heat transfer coefficient inside the room. The subscript $_{-j}$ indicates the direction of the walls. The subscripts $_{-set}$ and $_{-o}$ refer to the set value of air-conditioning system and outside air, respectively. V_{oa} is the volume of outdoor air, C_{air} is the specific heat of the air and γ_{air} is the specific weight of the air.
Building latent heat load H_l is expressed as:

$$H_l = S_f V_{oa} \gamma_{air} (X_{set} - X_o) + S_f W_l \cdots\cdots (15)$$

W_l represents the internal latent heat generation.
Finally anthropogenic heat from building HVAC systems can be written as:

$$Q_S = rat \cdot \left(1 + \frac{1}{COP}\right) \sum_i^{all} (H_{S,i} + H_{l,i}) \cdots\cdots\cdots (16)$$

COP is mechanical performance of air-conditioning system, *rat* is a ratio of sensible heat disposal to total at an exterior air-conditioning equipment like a cooling tower and so on.
Qs is split into two halves, and each of them is assumed to be exhausted from two heights. One is a close point to ground surface and the other is top of the building.

RESULTS OF STANDARD SOLUTION

Table 1 shows the basic assumption for standard calculation type. Geometric figures of the street were determined by statistical numbers came from the results of investigation at Marunouchi, Tokyo (Ojima Laboratory of Waseda University 1994) that is one of

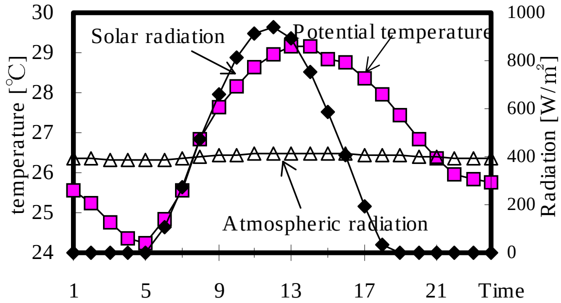

Fig.6 Boundary conditions

Table 1 Basic assumption

Wall	plaster board(9mm)+insulation (25mm)+concrete(200mm)+tile
Glass	6mm, ratio of glazing 30%
Covering ratio	asphalt pavement : soil : lawn = 1 : 1 : 1
Solar radiation reflectivity	building wall : 0.4, soil : 0.2 asphalt pavement : 0.2, lawn:0.2
Street configuration	building width B=32m, road width W=19m, building height H=24m, floor area ratio :750%
Setting of air-conditioning	26°C,RH50% constant (8:00 - 21:00)
COP of air-conditioning system	3
Exterior air-conditioning equipment	disposed sensible heat proportion sensible : latent =1:1 (rat=0.5)
Anthropogenic heat from traffic (at the peak)	10W per square meter of the area of the block
Internal heat generation of building (at the peak)	sensible heat: 53W per square meter of the area of the room latent heat : 13W per square meter of the area of the room

the most representative office district in Japan. Figure 6 indicates the boundary conditions of potential temperature, solar radiation and atmospheric radiation at the height of 150 meters, top of the Surface Boundary Layer (SBL). Wind velocity and absolute humidity at the boundary are 5 m/s and 19.3g/kg constant respectively. These values based on the measurement data assumed a typical urban area during summer season (Ishino 1995). Little statistical measurement data expressed by the potential temperature is available. And it seems not to be significant if the temperature is substituted for the potential temperature under the assumed conditions in the present study. Those are why we adopted the measurement data of air temperature.
Anthropogenic heat from traffic and building internal heat gain are defined by time series data, also based on the former investigation (Ichinose 1994). The assumption of the amount of precipitation is 25 mm per day which occurs once per 10 days, that is, rainfalls are assumed to be on 1st, 11th and 21st day. Calculation results of 20th day (the day before precipitation) and 22nd (the day after precipitation) are considered for following discussion.

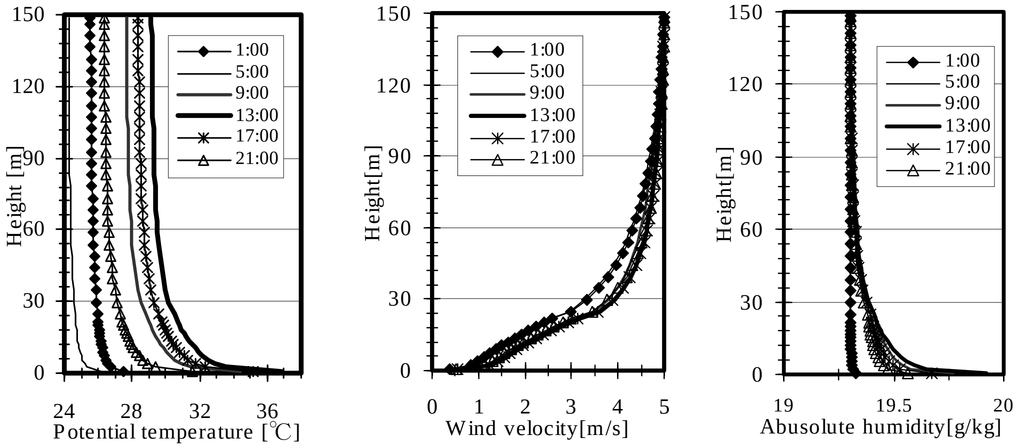

Fig.7 Vertical distribution of results of the standard case with basic assumption in a day after rainfall

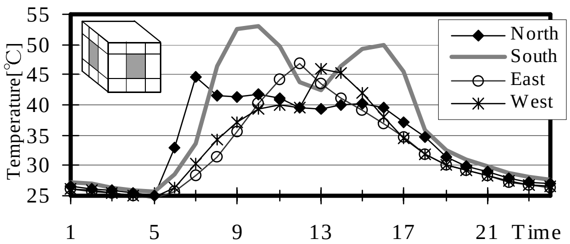

Fig.8 Fluctuaion of wall surface temperature in a day after rainfall

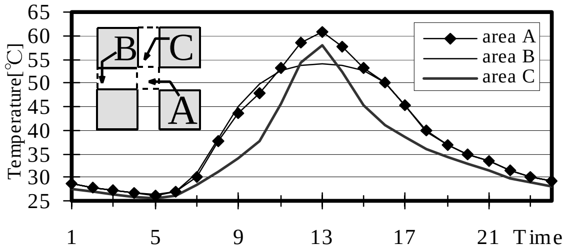

Fig.9 Fluctuation of surface temperature of asphalt pavement in a day after rainfall

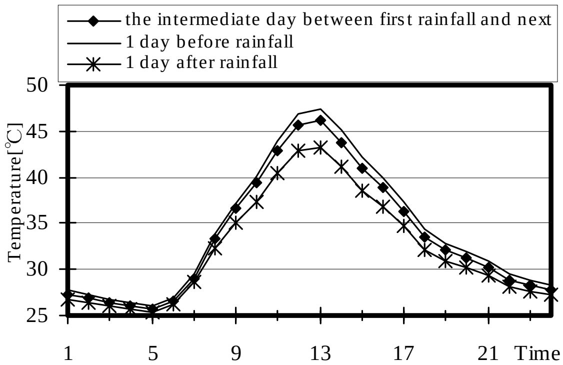

Fig.10 Fluctuation of surface temperature of soil

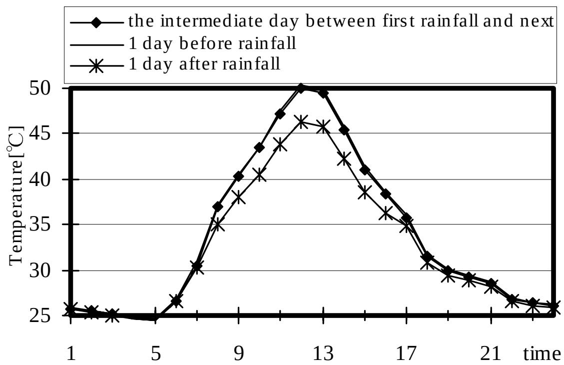

Fig.11 Fluctuation of surface temperature of lawn

Figure7 shows the results of the vertical distributions of potential temperature, wind velocity and absolute humidity.

The profiles of potential temperature and absolute humidity near the ground surface fluctuate intensively as compared with those near the top of SBL. The profile of wind velocity changes remarkably around 26m, the height of building.

Figure 8 shows the daily fluctuations of surface temperature of the walls.

Figure 9, 10 and 11 shows the calculation results of surface temperature of asphalt pavement, soil and lawn, respectively. Surface temperatures of both soil and lawn after precipitation are lower by about 5 degrees than those before precipitation at the peak of the day.

NUMERICAL EXPERIMENT

Using BUSSSM, numerical experiment is performed. As supposed significant factors of the heat island phenomenon, 11 factors such as ground materials, geometric urban configuration, artificial exhausted heat release, physical properties of buildings envelop, mechanical performance of air-conditioning system and so forth were selected out. The number of computation cases is 24.

Table 2 shows the result of numerical experiments. The average, maximum and minimum potential temperatures at the height of 2.4m are adopted for evaluation.

Table 2　Result of numerical experiment

Factors and levels		Potential temperature at the height of 2.4m [℃]					
		Average		Maximum		Minimum	
			difference		difference		difference
Covering proportion asphalt : soil : lawn	1:0:0	29.77	+0.13	33.86	+0.24	25.41	+0.06
	1:1:1	29.64		33.62		25.35	
	0:1:0	29.58	-0.06	33.46	-0.16	25.35	+0.00
	0:0:1	29.58	-0.06	33.54	-0.08	25.29	-0.06
Street configuration (floor area ratio)	750%	29.64		33.62		25.35	
	1000%	29.39	-0.25	33.19	-0.43	25.27	-0.08
	1500%	29.16	-0.48	32.79	-0.83	25.21	-0.14
Reflectivity of solar radiation	0.4	29.68	+0.04	33.66	+0.04	25.37	+0.02
	0.6	29.64		33.62		25.35	
	0.8	29.61	-0.03	33.59	-0.03	25.33	-0.02
Internal heat generation	sensible 56W/m^2 latent 13W/m^2	29.64		33.62		25.35	
	sensible 84W/m^2 latent 20W/m^2	29.81	+0.17	33.89	+0.27	25.36	+0.01
	sensible 112W/m^2 latent 26W/m^2	29.94	+0.30	34.13	+0.51	25.36	+0.01
	sensible 140W/m^2 latent 33W/m^2	30.08	+0.44	34.35	+0.73	25.37	+0.02
Anthoropogenic heat from traffic	10W/m^2	29.64		33.62		25.35	
	20W/m^2	29.70	+0.06	33.69	+0.07	25.39	+0.04
	40W/m^2	29.81	+0.17	33.81	+0.19	25.47	+0.12
Operation of air-conditioning system	intermittent	29.64		33.62		25.35	
	continuous	29.77	+0.13	33.60	-0.02	25.61	+0.26
COP of air-conditioning system	2	29.69	+0.05	33.70	+0.08	25.35	+0.00
	3	29.64		33.62		25.35	
	4	29.62	-0.02	33.58	-0.04	25.35	-0.00
	5	29.61	-0.03	33.56	-0.06	25.35	-0.00
sensible heat factor of exhaust heat at exterior air-conditioning equipment (sensible heat:latent heat)	1:0	29.97	+0.33	34.21	+0.59	25.36	+0.01
	2:1	29.76	+0.12	33.82	+0.20	25.36	+0.01
	1:1	29.64		33.62		25.35	
	0:1	29.28	-0.36	32.97	-0.65	25.33	-0.02
Insulation	no insulation	29.62	-0.02	33.61	-0.01	25.31	-0.04
	depth 25mm	29.64		33.62		25.35	
	50mm	29.65	+0.01	33.62	+0.00	25.36	+0.01
Ratio of glazing	10%	29.76	+0.12	33.69	+0.07	25.48	+0.13
	30%	29.64		33.62		25.35	
	50%	29.53	-0.11	33.56	-0.06	25.23	-0.12
Object of discussion related rainfall schedule	the day after rainfall	29.64		33.62		25.35	
	the day before rainfall	29.68	+0.04	33.70	+0.08	25.37	+0.02

(shaded) standard case with basic assumption in Table1

\+ indicates higher temperature of the case than that of standard case

\- indicates lower temperature of the case than that of standard case

Generally speaking, effects of street configuration, sensible heat factor of exhaust heat, ratio of glazing and covering proportion are significant. The reason of potential temperature decrease with increasing of the floor area ratio is probably effect of the buildings sunshade, which causes notable reduction of building surface temperature.

The larger area of glazing makes both larger building thermal load and lower surface temperature of the building. Consequently, the potential temperature decreases as ratio of glazing area increases, especially at night.

Outstanding effects to increase both average and maximum potential temperatures are recognized on the factors of internal heat generation and sensible heat factor of exhaust heat at exterior air-conditioning equipment. On the other hands, regarding to the minimum potential temperature, operating time of air-conditioning system is dominant.

Looking at the insulation of the wall, its effect on the potential temperature is relatively small.

CONCLUTION

The analysis in the present work leads to the following conclusions.

1. Building-Urban-Soil Simultaneous Simulation Model (BUSSSM) was proposed, which is able to describe complex simultaneous problems observed in urban area, related to the heat island phenomenon. The result of standard case with basic assumption was obtained.
2. Significant effects to cut down average, maximum and minimum potential temperature are observed on the factors of street configuration, sensible heat factor of exhaust heat glazing area and ground materials.
3. The factors of internal heat generation and sensible heat factor of exhaust heat act significantly to raise both average and maximum potential temperature.
4. The potential temperature decreases distinctively at nighttime, as the ratio of glazing area increases.

ACKNOWLEDGEMENTS

The authors sincerely appreciate Prof. Hayashi of Kyushu University who was willing to guide us through a bunch of discussions serving to describe about the physical concepts. Also thanks to many students of our laboratory, contributed to the progress of this study facing their masters' theses.

REFERENCE

Roger A. Pielke: Mesoscale Meteorological Modeling, ACADEMIC PRESS, p.159, London (1990)

Takashi Maruyama: Numerical calculation of turbulent boundary layer using refined k-ε model in consideration of drag and volume change of roughness elements, Transaction of AIJ, No.404, p.75-81 (1989.10) (in Japanese)

Jun Tanimoto, Tetsuo Hayashi and Tadahisa Katayama: A Study on simplified calculation procedure for evaporation rate from soil covered construction, Transaction of AIJ, No.492 p.23-29 (1997.2) (in Japanese)

Takako Kawakami, Tadahisa Katayama, Jun Tanimoto and Aya Hagishima: Study on a simplified calculation procedure of estimation for evaluation rate from soil surface, part6 proposition of a revised model taken account of hdroulic conductivity and diffusion, AIJ Kyushu Chapter Architectural Research Meeting (Environment), No.37-2, p.205-208 (1999.3) (in Japanese)

Harumi Kagawa, Tetsuo Hayashi, Jun Tanimoto and Tadahisa Katayama: Study on effect of lawn surface on thermal environment in urban area, Transaction of AIJ, No.507,p.7-12 (1998.5) (in Japanese)

Ojima Laboratory of Waseda University: Comparison of geometric urban configuration (1994)(in Japanese)

Hisaya Ishino, Masakazu Moriyama, Kitarou Mizude and Satoshi Nakayama: A Study on analysis about urban thermal environment by numerical simulation using 1-dimensional heat balance model and survey of near the ground thermal conditions, Transaction of AIJ, No.469, p.45-51 (1995.3)(in Japanese)

Toshiaki Ichinose, Keisuke Hanaki, Tomonori Matsuo: Analyses on Geographical Distribution of Urban Anthropogenic Heat Based on Very Precise Geographical Information, Proc. of Environmental Engineering Research, Vol.31, p.263-273 (1994)(in Japanese)